



Transactions of the 13th International Conference on Structural Mechanics in Reactor Technology (SMiRT 13), Escola de Engenharia - Universidade Federal do Rio Grande do Sul, Porto Alegre, Brazil, August 13-18, 1995

## Shear-bending buckling strength of FBR main vessels

Matsuura, S.<sup>1</sup>, Nakamura, H.<sup>1</sup>, Kawamoto, Y.<sup>2</sup>, Murakami, T.<sup>3</sup>, Ogiso, S.<sup>4</sup>, Akiyama, H.<sup>5</sup>

1) *Central Research Inst. of Electric Power Industry, Abiko, Japan*

2) *Mitsubishi Heavy Industries, Ltd., Nagasaki, Japan*

3) *Toshiba Corporation, Yokohama, Japan*

4) *Kawasaki Heavy Industries, Ltd., Tokyo, Japan*

5) *University of Tokyo, Tokyo, Japan*

**ABSTRACT:** Buckling under earthquake loading is one of the most important problem for FBR main vessels of thin wall thickness. Therefore, many tests using cylinder model made of stainless steel and FEM calculations corresponding to those tests were carried out. Based on the results of buckling tests and numerical calculations, shear-bending buckling strength evaluation formulae are developed and the usefulness of numerical methods are clarified.

### 1 INTRODUCTION

Buckling under earthquake loading is one of the most important problem for FBR main vessels of thin wall thickness. Therefore, Central Research Institute of Electric Power Industry (CRIEPI, Japan), commissioned by the Ministry of International Trade and Industry of the Japanese government, has been carried out the demonstration test and research program of major parameters of FBR main vessels for buckling evaluation varies as follows:

Radius (R) to thickness (t) ratio;  $R/t=50 \sim 400$

Length (L) to radius (R) ratio;  $L/R=1.0 \sim 5.0$

Cylinder root bending stress to shear stress ratio;  $H/R=1.0 \sim 5.0$

Material; Type 304 and 316 stainless steel

Temperature; Room temperature to 550 °C

A cylinder subjected horizontal load under such conditions as shown above can fail by elastic-plastic buckling in shear or in bending. Many tests using cylinder model made of stainless steel and FEM calculations corresponding to those tests were carried out. Then, shear and bending buckling strength evaluation formulae were investigated and the accuracy of calculation was examined.

### 2 PREVIOUS STUDIES OF SHEAR-BENDING BUCKLING OF CYLINDRICAL SHELLS

Although large amount of investigations on buckling problems of cylindrical shells have been carried out, investigations on shear-bending buckling of short cylindrical shells under transverse shearing loads were few. Shear-bending buckling experiments using cylindrical models made of steel and aluminum alloy have been carried out by

Lundquist (1935), by Galletly and Blachut (1985), by Akiyama et al. (1987), by Choi et al. (1986), by Dostal et al. (1987) and by Okada et al. (1993). Among them, the experiments by Galletly and Blachut (1985), by Dostal et al. (1987) and by Okada et al. (1993) were aimed to apply to FBR.

The buckling strength evaluation formulae for elastic torsional buckling is derived by Timoshenko and Gere (1961) and by Yamaki (1984) theoretically, which are used in ASME Code Case N-284 and work of Galletly (1985).

### 3 STATIC BUCKLING TESTS AND NUMERICAL ANALYSES

We conducted buckling tests using fabricated stainless steel cylinder models at room and elevated temperatures (by Matsuura et al. (1991), by Murakami et al. (1993) and by Ogiso et al. (1993)). Figure 1 shows the schematic view of shear-bending buckling test setup. Transverse shearing loads are applied by the screw jack to the upper flange of the specimen fixed on the floor. The ratio of H/R corresponds to the ratio of maximum axial stress at cylinder root to maximum shear stress at shell wall, which are induced by transverse shearing force.

We also carried out numerical analyses to simulate typical buckling tests using Finite Element Codes, where plasticity and geometrical nonlinearities are taken into account. The buckling strength obtained by numerical simulations is shown in Fig. 2, normalized by the experimental buckling strength. The buckling strength obtained by numerical analyses are from 0% to 20% greater than that of experiments. This shows that the numerical analysis is a useful tool for evaluating buckling strength. However, appropriate mesh division and consideration of initial shape imperfections are necessary to obtain accurate buckling strength (by Matsuura et al. (1995)).

We calculate the nonlinearity factor  $\mu$ , which represents nonlinear effect of plasticity on load-displacement relation before the buckling point as shown in Fig. 3. The values of  $\mu-1$  obtained by numerical analyses are shown in Fig. 4 compared with experimental values. From this figure, numerical results are larger than experimental results and vary within two times as large as experimental values.

### 4 BUCKLING STRENGTH EVALUATION FORMULAE

#### 4.1 Shear Buckling Strength Evaluation Formulae

Theoretical torsional buckling formula of a cylindrical shell has been given by Timoshenko and Gere (1961). It is well known that the elastic torsional buckling formula gives more conservative stress evaluation than elastic shear buckling, yielding almost the lower limit of the experimental values of shear buckling (see Fig. 5). Taking into account the data scattering, especially in the elastic buckling range, the torsional buckling formula multiplied by a coefficient of 0.8 is adopted as the elastic shear buckling stress ( $\tau_{cr}^e$ ) formula. The plastic buckling stress ( $\tau_{cr}^p$ ) is evaluated using the interaction relation of the yield stress with the elastic buckling stress. The allowable shear buckling strength ( $Q_{at}$ ) can be obtained by converting shear stress to transverse load, which has been divided by the strength safety factor to take into account the uncertainty of buckling strength

(see Eqs.(1),(2),(3)).

$$\tau_{cr}^e = 0.8 \frac{4.82}{\left(\frac{L}{\sqrt{Rt}}\right)^2} \sqrt{1 + 0.0239 \left(\frac{L}{\sqrt{Rt}}\right)^3} \frac{Et}{R} \quad (1)$$

$$\frac{\tau_{cr}^p}{\tau_{cr}^e} + \left( \frac{\sqrt{3} t_{cr}^p}{1.27 S_y} \right)^2 = 1 \quad (2)$$

$$Q_a = \tau_{cr}^p \pi R t \frac{1}{v_s} \quad (3)$$

where  $E$  is Young's modulus,  $S_y$  is design yield stress,  $v_s$  is the strength safety factor for shear buckling.

Various methods are available for considering the influence of plasticity. Nevertheless, the plasticity reduction relation shown in Eq. (2) has been employed, which is relatively simple, smoothly connectable from the elastic range to the plastic range and in close agreement with test results.

#### 4.2 Bending Buckling Strength Evaluation Formulae

The NASA design formula (NASA SP-8007 (1968)), highly reliable as an elastic bending buckling stress ( $\sigma_{b,cr}^e$ ) formula, is adopted to evaluate elastic-plastic bending buckling stress ( $\sigma_{b,cr}^p$ ) by the same procedure as for the shear buckling strength.

Figure 6 shows the relation of evaluated elastic bending buckling stress values to elastic buckling test data (JEAG4601 (1984)). From the Fig. 6, it may be recognized that the formulae give more conservative value than 95% lower-confidence limit of the test data.

The allowable bending buckling strength ( $M_{al}$ ) can be obtained by converting the above-mentioned elastic-plastic bending buckling stress to bending moment, which has been divided by the strength safety factor to take into consideration of the uncertainty of bending buckling strength (see Eqs. (4),(5),(6)).

$$\sigma_{b,cr}^e = 0.6 \times \left[ 1 - 0.731 \times \left\{ 1 - \exp\left( -\frac{1}{16} \sqrt{\frac{R}{t}} \right) \right\} \right] \frac{Et}{R} \quad (4)$$

$$\frac{\sigma_{b,cr}^p}{\sigma_{b,cr}^e} + \left( \frac{\sigma_{b,cr}^p}{1.27 S_y} \right)^2 = 1 \quad (5)$$

$$M_{al} = \sigma_{b,cr}^p \pi R^2 t \frac{1}{v_b} \quad (6)$$

where  $v_b$  is the strength safety factor for bending buckling.

#### 4.3 Axial Buckling Strength Evaluation Formulae

We adopt the NASA design formula for axial compression buckling stress ( $\sigma_{a,cr}^e$ ) and the same procedure as previously mentioned, and the allowable buckling strength ( $F_{al}$ ) for axial compression can be obtained (see Eqs. (7),(8),(9)). These formulae are mainly intended to obtain the axial compression buckling strength for evaluating the effects of additional axial force on shear-bending buckling.

$$\sigma_{a,cr}^e = 0.6 \times \left[ 1 - 0.901 \times \left\{ 1 - \exp\left( -\frac{1}{16} \sqrt{\frac{R}{t}} \right) \right\} \right] \frac{Et}{R} \quad (7)$$

$$\frac{\sigma_{a,cr}^p}{\sigma_{a,cr}^e} + \left( \frac{\sigma_{a,cr}^p}{S_y} \right)^2 = 1 \quad (8)$$

$$F_{al} = \sigma_{a,cr}^p 2\pi R t \frac{1}{v_c} \quad (9)$$

where  $v_c$  is the strength safety factor for axial compression buckling.

#### 4.4 Interaction between Shear Buckling and Bending Buckling, and Additional Effects of Axial Loads on Them

Buckling modes obtained by experiments are shown in Fig. 7. It is clear from the figure that the dominant buckling mode, which is shear or bending, depends on geometrical parameters.

To confirm the seismic stability related to buckling phenomena, it is necessary to consider the interaction of shear, bending and axial buckling modes. The FBR main vessels considered in the present paper, however, are hung from a roof deck, and normally, tensile stress in the vertical direction exists in them due to gravity. Therefore, the axial force caused by vertical seismic load may be recognized as additional force leading to the occurrence of shear-bending buckling.

After studying the various methods to consider the interaction effects, we selected the following formulae.

$$\left[ \left\{ \frac{Q}{Q_{al}} \right\}^5 + \left\{ \frac{M}{M_{al}} + \frac{F}{F_{al}} \right\}^5 \right] < 1 \quad \left( \begin{array}{l} F \geq 0 : \\ \text{(Compressive force)} \end{array} \right) \quad (10)$$

$$\left[ \left\{ \frac{Q}{Q_{al}} \right\}^5 + \left\{ \frac{M + \frac{ZF}{A}}{M_{al}} \right\}^5 \right] < 1 \quad \left( \begin{array}{l} F < 0 : \\ \text{(Tensile force)} \end{array} \right) \quad (11)$$

where A is cross-sectional area of cylinder, Z is section modulus of cylinder, Q is applied transverse shear load, M is applied bending moment and F is applied axial force.

The linear interaction relation is adopted for the combination of bending moment and axial force. As for the combination of shear and bending, interaction effects of the fifth power are adopted.

Comparisons of these formulae with the test results are plotted in Figs.8 and 9. The 95% lower-confidence limit of the buckling test data is greater than the buckling strength evaluated by present formulae (where  $\nu_s = \nu_b = 1.0$ ).

## 5 CONCLUSIONS

Based on the results of various buckling tests and analyses, the formulae for evaluating shear-bending buckling strength of the FBR main vessel were presented. Shear buckling and bending buckling were evaluated under the assumption that both buckling modes slightly interact with each other. Plasticity reduction was performed using the interaction relation which is linear for elastic buckling stress and quadratic for yield stress. The formulae give the moderately conservative buckling strength.

This study forms a part of the "Demonstration Test and Research Program of Buckling" of the Ministry of International Trade and Industry (MITI) of Japanese government.

## REFERENCES

- Akiyama, H., Takahashi, M. and Hashimoto, S., Buckling tests of steel cylindrical shells subjected to combined bending and shear, Trans. of Architectural Institute of Japan, (in Japanese), No.371, (1987), pp.44-51.
- Choi, H.S., Tanami, T. and Hangai, Y., Failure tests of cantilevered cylindrical shells under a transverse load, Trans. of Architectural Institute of Japan, (in Japanese), No.369, (1986), pp.60-69.
- Dostal, M., Austin, N., Combescure, A., Peano, A. and Angeloni, P.: Shear buckling of

cylindrical vessels benchmark exercise, SMiRT-9, Vol. E, 1987, pp.199-208

Galletly, G. D. and Blachut, J., Plastic buckling of short vertical cylindrical shell subjected to horizontal edge shear loads, Journal of Pressure Vessel Tech., Vol.107, (1985), pp.101-106.

Lundquist, E.E., Strength tests of thin-walled duralumin cylinders in combined transverse shear and bending, NACA-TN-No.523, (1935).

Matsuura, S., Nakamura, H., Ogiso, S., Ooka, Y. and Akiyama, H., Buckling strength evaluation of FBR main vessels under lateral seismic loads, 11th SMiRT, vol.E, (1991), pp. 269-280.

Matsuura, S., Nakamura, H., Kokubo, K., Ogiso, S. and Ohtsubo, H., Shear-bending buckling analyses of fast breeder reactor main vessels, Nuclear Engineering and Design 153, (1995),pp. 305-317

Murakami, T., Yoguchi, H., Hirayama, H., Nakamura, H. and Matsuura, S., The effects of geometrical imperfection on buckling strength of cylindrical shells in bending, 12th SMiRT, vol. E, (1993), pp.257-268

NASA SP-8007, Buckling of Thin-Walled Circular Cylinders, (1968).

Ogiso, S., Sasaki, T., Ooka, Y., Nakamura, H. and Akiyama, H., Cyclic post-buckling tests for low cycle fatigue failure of buckled cylinders by shear and bending modes, 12th SMiRT, vol.E, (1993), pp. 287-292

Okada, J., Iwata, K., Tsukimori, K. and Nagata, T., An Evaluation method for plastic buckling of circular cylindrical shells under shear forces, 12th SMiRT, Vol.E, (1993), pp.281-286.

The Japan Electric Association, Technical Guidelines for Aseismic Design of Nuclear Power Plants (JEAG4601) (in Japanese), (1984).

Timoshenko, S.P. and Gere, J.M., Theory of Elastic Stability, (1961), McGraw-Hill Book Co.

Yamaki, N., Elastic Stability of Circular Cylindrical Shells, (1984), North-Holland.

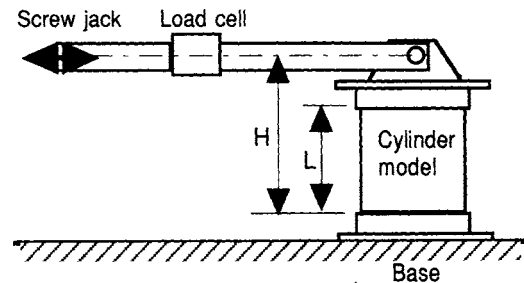


Fig. 1 Schematic view of shear-bending buckling test setup

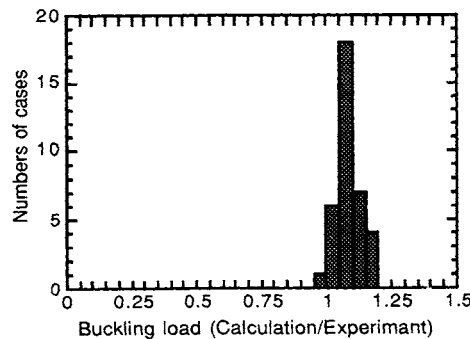


Fig. 2 Buckling strength results of numerical analyses

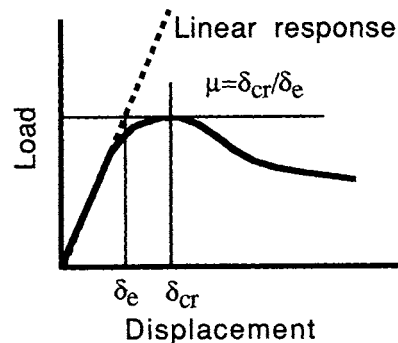


Fig. 3 Nonlinearity factor  $\mu$

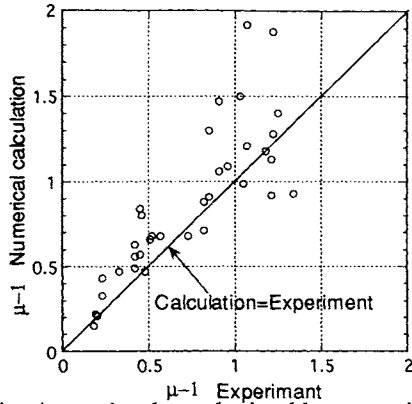


Fig. 4  $\mu - 1$  values obtained by numerical analyses

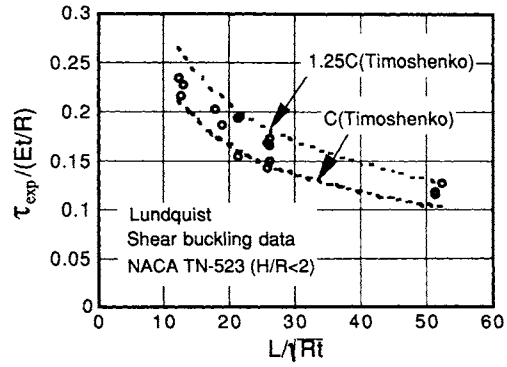


Fig. 5 Comparison of torsional buckling evaluation formula by Timoshenko and elastic shear buckling test results by Lundquist

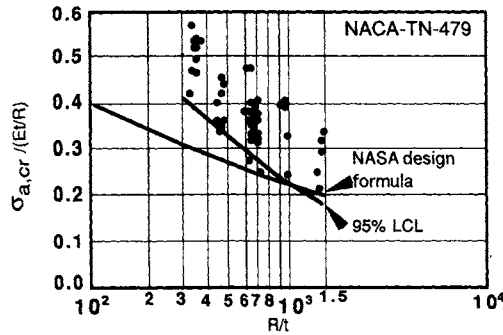


Fig. 6 Comparison of NASA design formula and elastic bending buckling results by Lundquist

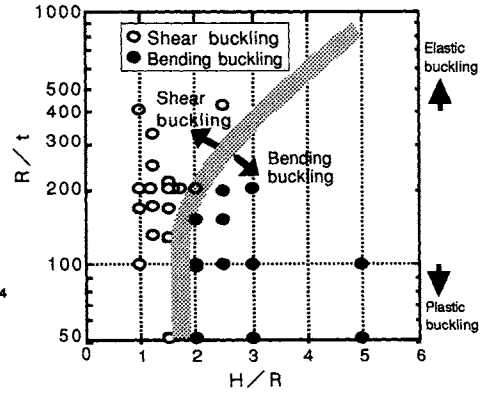


Fig. 7 Buckling modes obtained by experiments

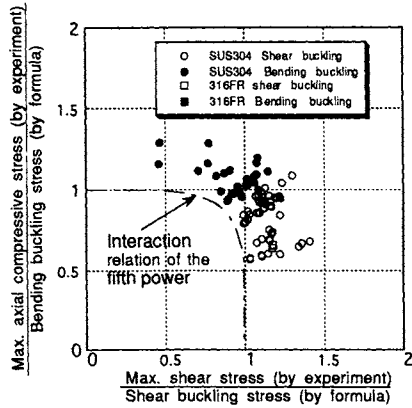


Fig. 8 Interaction relation between shear buckling and bending buckling

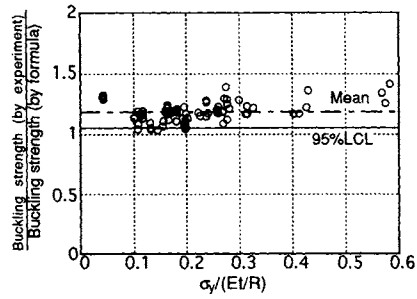


Fig. 9 Buckling strength evaluated by present formulae